Journal of the European Ceramic Society 20 (2000) 2421–2425

Chemical compatibility of $RE_{0.6}M_{0.4}Mn_{0.8}Co_{0.2}O_{3-\delta}$ (RE = La, Pr, Nd, Sm and Gd; M = Sr and Ca) with yttria stabilized zirconia

H.Y. Tu *, W.Y. Sun, Y.J. Yang, Z.Y. Lu, D.Q. Wang, T.L. Wen

Shanghai Institute of Ceramics, Chinese Academy of Sciences, 1295 Ding Xi Road, Shanghai 200050, People's Republic of China

Received 25 October 1999; accepted 11 April 2000

Abstract

The chemical compatibility of one new series, $RE_{0.6}M_{0.4}Mn_{0.8}Co_{0.2}O_{3-\delta}$ (RE = La, Pr, Nd, Sm and Gd; M = Sr and Ca), with yttria stabilized zirconia (YSZ) has been examined. Powder mixtures of perovskites and YSZ were annealed at 1200° for 24h in air. $RE_{0.6}M_{0.4}Mn_{0.8}Co_{0.2}O_{3-\delta}$ showed different compatibility towards YSZ for M = Sr and Ca, respectively. The formation of $SrZrO_3$ was identified by X-ray diffraction analysis as a reaction product for $RE_{0.6}Sr_{0.4}Mn_{0.8}Co_{0.2}O_{3-\delta}$. In contrary, there is no reaction product for $RE_{0.6}Ca_{0.4}Mn_{0.8}Co_{0.2}O_{3-\delta}$. EDX analysis revealed that there is a larger difference between the solubility of Sr and Ca in YSZ. The bond-valence model was used to discuss the different compatibility of Sr and Ca series perovskites with YSZ. The present studies also showed that the formation of $SrZrO_3$ was favored for larger disorder effect due to size difference between A-site RE^{3+} and Sr^{2+} in $RE_{0.6}Sr_{0.4}Mn_{0.8}Co_{0.2}O_{3-\delta}$.

Keywords: Chemical compatibility; Diffusion; Fuel cells; Perovskite; (RE, M) $(Mn, Co)O_3$; ZrO_2

1. Introduction

The solid oxide fuel cell (SOFC) represents a promising clean and efficient power generation technology. Therefore, SOFC has recently attracted great attention in the world. One of the current trends is the reduction in operating temperature for the practical application of SOFC. An operating temperature in the range $600°C < T < 800°C$ could result in the use of an oxidation-resistant stainless steel or another alloy as the interconnect material. The reduction in operating temperature would also reduce operating costs, increase durability, extend service life, and permit more frequent cycling. However, the overpotentials of the cathode significantly increase with decreasing operating temperature. For this purpose, Ishihara et al.[1] investigated the cathodic characteristics of $RE_{0.6}Sr_{0.4}MnO_3$ (RE is La, Pr, Nd, Sm, Gd, Yb and Y). The overpotential of the cathode for oxygen reduction decreased in the following order: Y > Yb > La > Gd > Nd > Sm > Pr at 1000°. $Pr_{0.6}Sr_{0.4}MnO_3$ also exhibits lower overpotential than $La_{0.6}Sr_{0.4}MnO_3$ in a low-temperature range.

Although some other rare earth manganites exhibit lower cathodic overpotential than La manganites, the electrode performance of these rare earth manganites needs to be improved further. It is indicated by Tu et al.[2] that substitution of Mn by a moderate amount of Co can improve the electrode performance, without causing thermal expansion mismatch and reactivity with YSZ electrolyte. For the development of a new cathode with low overpotential in the reduced temperature region, the chemical compatibility between the cathode and YSZ electrolyte is highly important for the fabrication and operation of the SOFC. In the present study, the chemical compatibility of one new series, $RE_{0.6}M_{0.4}Mn_{0.8}Co_{0.2}O_{3-\delta}$ (RE = La, Pr, Nd, Sm and Gd; M = Sr and Ca), with YSZ has been examined.

2. Experimental

The perovskite-type oxides, $RE_{0.6}M_{0.4}Mn_{0.8}Co_{0.2}O_{3-\delta}$ (RE = La, Pr, Nd, Sm, Gd; M = Sr and Ca), were prepared from La_2O_3(99.99%), Pr_6O_{11}(99.9%), Nd_2O_3 (99.9%), Sm_2O_3(99.9%), Gd_2O_3(99.95%), $SrCO_3$(99.0%), $CaCO_3$ (99.0%), MnO_2(99.0%) and Co_2O_3(99.0%). The starting powders were thoroughly mixed in the appropriate ratio

* Corresponding author. Fax: +86-216-251-3903.
E-mail address: heyotu@online.sh.cn (H.Y. Tu).

0955-2219/00/$ - see front matter
PII: S0955-2219(00)00126-6

under absolute alcohol, using an agate mortar and pestle, and calcined at 1000°C for 12 h in air. The calcined samples were then ground, pressed into pellets, and finally synthesized at 1300°C for 10 h in air. The specimens for the reaction study were prepared by mixing thoroughly the as-synthesized perovskites and YSZ powders (8 mol% Y_2O_3 stabilized zirconia, Tosoh, Japan) in a 1:1 weight ratio, and then pressing the powder mixtures into a pellet. The pellets were annealed at 1200°C for 24 h in air. This temperature corresponds to that of fabrication of cathodes. Characterization of the as-synthesized perovskites and reaction products was performed using X-ray powder diffraction (XRD) on a Rigaku-RC (12 kW) diffractometer with monochromated CuKα radiation and a scintillation detector. The La-based perovskites were chosen to study oxygen vacancy, weight loss, phase transformation and ion interdiffusion. The oxygen content of the as-synthesized perovskites was checked by iodometric titration using an aqueous solution of sodium thiosulfate as a standard solution. The thermogravimetric analysis (TGA) and differential thermal analysis (DTA) were performed from room temperature to 1200°C in air at rate of 5°C/min with Simultaneous Thermal Analyzer STA 429 Netzsch GerMtebau GmbH. The chemical composition of the phases present in the samples after annealing was measured using energy dispersive X-ray spectroscopy (EDX) (Link ISIS).

3. Results

The observed phases are summarized in Table 1 for $RE_{0.6}M_{0.4}Mn_{0.8}Co_{0.2}O_{3-\delta}$ (RE = La, Pr, Nd, Sm and Gd; M = Sr and Ca). All the compositions showed highly distorted orthorhombic symmetry at ambient temperature. The XRD patterns were indexed on the basis of the $GdFeO_3$ type with orthorhombically distorted perovskite structure (space group Pbnm). For the different compositions, a lattice effect is the random disorder of RE^{3+} and A^{2+} cations with different sizes distributed over the A sites in the perovskite structure. The weighted average A-site cation radius $<r_A>$ was used to quantify this effect. Standard ionic radii with values for ninefold coordination in oxides[3] were used to calculate $<r_A>$. These $<r_A>$ values are also listed in Table 1.

Table 1
The cell parameters and average A-site cation radius for $RE_{0.6}M_{0.4}Mn_{0.8}Co_{0.2}O_{3-\delta}$ (RE = La, Pr, Nd, Sm and Gd; M = Sr and Ca)

$RE_{0.6}A_{0.4}$	a (Å)	b (Å)	c (Å)	$<r_A>$ (Å)
$La_{0.6}Sr_{0.4}$	5.463	5.541	7.741	1.25
$Pr_{0.6}Sr_{0.4}$	5.463	5.487	7.690	1.23
$Nd_{0.6}Sr_{0.4}$	5.463	5.494	7.681	1.22
$Sm_{0.6}Sr_{0.4}$	5.435	5.444	7.677	1.20
$Gd_{0.6}Sr_{0.4}$	5.478	5.424	7.661	1.19
$La_{0.6}Ca_{0.4}$	5.439	5.507	7.686	1.20
$Pr_{0.6}Ca_{0.4}$	5.405	5.564	7.642	1.18
$Nd_{0.6}Ca_{0.4}$	5.404	5.464	7.628	1.17
$Sm_{0.6}Ca_{0.4}$	5.406	5.463	7.587	1.15
$Gd_{0.6}Ca_{0.4}$	5.336	5.481	7.542	1.14

The XRD patterns of the perovskite/YSZ mixtures, after annealing at 1200°C for 24 h, are shown in Fig. 1(a) and (b) for Sr and Ca series, respectively. $SrZrO_3$ is the unique reaction product, which is identified in the Sr series. In comparison, there is no reaction product in the case of Ca series. The lattice parameters for the cubic YSZ phase after annealing are given in Fig. 2 in comparison with that of pure YSZ. The expanded lattices were found for all the powder mixtures. A semi-quantitative representation of the relative amount of $SrZrO_3$ was obtained using the ratio between the intensity values of 100% reflections for $SrZrO_3$ (121 reflection) and YSZ (111 reflection). The results are shown in Fig. 3 for different rare earth elements. As can be seen, the

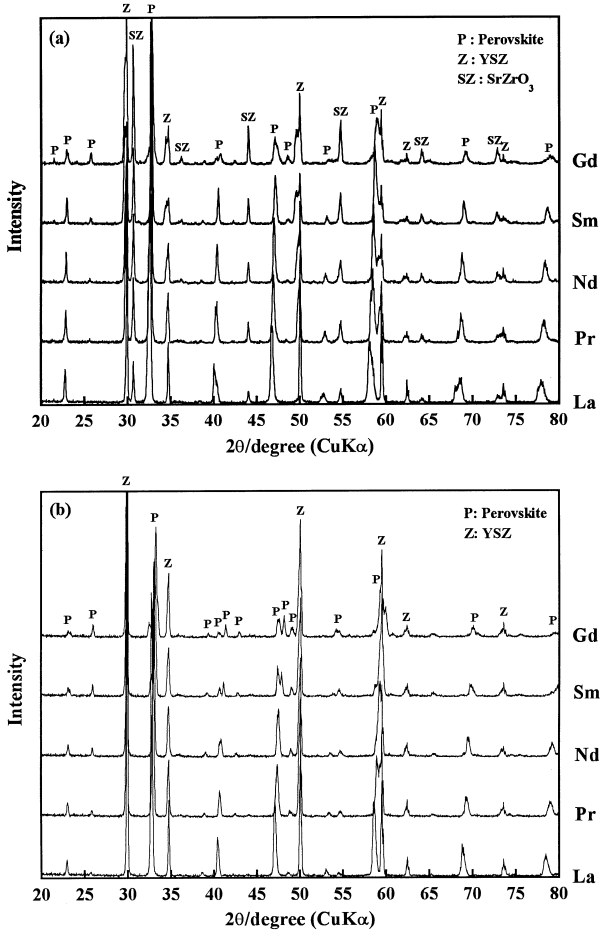

Fig. 1. X-ray powder diffraction patterns of $RE_{0.6}M_{0.4}Mn_{0.8}Co_{0.2}O_{3-\delta}$/YSZ mixtures after annealing at 1200°C for 24 h in air: (a) M = Sr and (b) M = Ca.

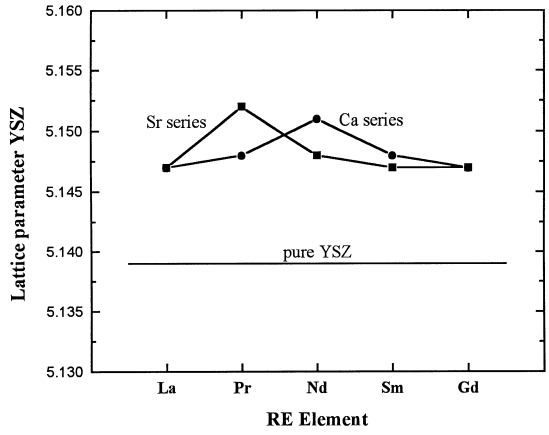

Fig. 2. Lattice parameters of the cubic YSZ phase for $RE_{0.6}M_{0.4}Mn_{0.8}Co_{0.2}O_{3-\delta}$/YSZ powder mixtures after annealing at 1200°C for 24 h in air (unit in Å).

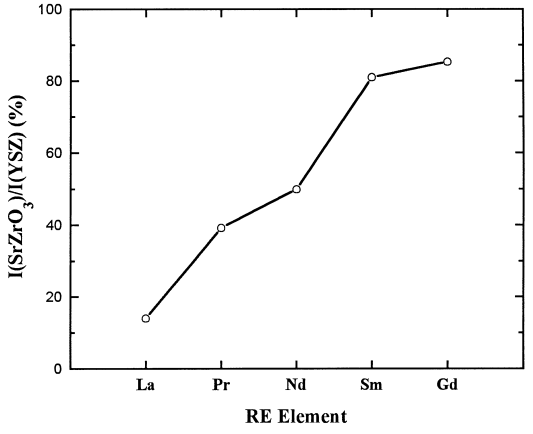

Fig. 3. Ratio of intensity values of the major XRD peaks of $SrZrO_3$ and YSZ as a function of RE element for $RE_{0.6}M_{0.4}Mn_{0.8}Co_{0.2}O_{3-\delta}$/YSZ powder mixtures after annealing at 1200°C for 24 h in air.

amount of $SrZrO_3$ formed increases with decreasing rare earth ionic radius.

The La-based perovskites were chosen to study B-site cation valence, oxygen vacancy, weight loss, phase transformation and ion interdiffusion, in order to identify the reasons of different chemical compatibility of Sr and Ca series with YSZ. Table 2 listed the results of iodometric titration, thermogravimetric analysis (TGA) and differential thermal analysis (DTA). As presented in Table 2, high concentrations of tetravalent Mn and Co were revealed by iodometric titration. Further, there were no indications of weight loss and phase transformation by TGA and DTA. This indicates that the same concentrations of tetravalent Mn and Co were maintained in the structures up to 1200°C.

The chemical compositions of the phase present in the two samples annealed at 1200°C were measured by EDX. The results are summarized in Table 3. The chemical analysis was performed on grains in the samples. The considerable interdiffusion between perovskites and YSZ was confirmed. Mn and Co were observed in YSZ for both the $LSMC(La_{0.6}Sr_{0.4}Mn_{0.8}Co_{0.2}O_{3-\delta})$/YSZ and $LCMC(La_{0.6}Ca_{0.4}Mn_{0.8}Co_{0.2}O_{3-\delta})$/YSZ mixtures. No La and Sr were observed in YSZ for the LSMC/YSZ mixtures, while La and Ca were observed in YSZ for the LCMC/YSZ mixtures. The perovskites in the two samples were found to contain 1–2 mol% Y and 7–15 mol% Zr.

4. Discussion

The different chemical compatibility of Sr and Ca series perovskites with YSZ may be explained by a combination of perovskite stability and ion diffusion. When a divalent acceptor M (M = Sr or Ca) is substituted for trivalent RE in $RE_{0.6}M_{0.4}Mn_{0.8}Co_{0.2}O_{3-\delta}$, the yielded structure violates the valence-sum rule in the bond-valence model described by Brown.[4] A fraction of B-site cations in ABO_3 perovskites is then converted from the trivalent to the tetravalent state in accordance with the valence-sum rule. As indicated in Table 2, a substantial fraction of B-site cations was converted from the trivalent to the tetravalent state in the perovskite structures of $La_{0.6}M_{0.4}Mn_{0.8}Co_{0.2}O_{3-\delta}$ (M = Sr or Ca).

At higher temperatures (up to 1200°C), the concentration of tetravalent state B-cations remained constant because no weight loss was observed in TGA which associated with the loss of lattice oxygen due to the transition of B-cations from tetravalent to trivalent states. As the temperature is raised, the atom in the structure will vibrate around its equilibrium position with increasingly large amplitude. Thus it will have some bonds that are larger and some shorter than the average bond length at any instant, leading to the distortion theorem prediction that the average bond length will be increased. As indicative of strained bonds, the discrepancy between cation valence and bond-valence sum around cation increases with temperature, leading to the instabilities of the tetravalent state of Mn and Co. In the annealing of perovskite/YSZ mixtures, unstable Mn^{4+} and Co^{4+} then diffused into the lattice of YSZ, leaving the perovskites B-site deficient. The existence of Mn and Co in YSZ, as confirmed in EDX analysis, can be considered to be due to the diffusion of unstable Mn^{4+} and Co^{4+} from LSMC and LCMC, respectively. The excess amounts of A-site cations will also leave the perovskite structure in accordance with the valence-sum rule. Solid solubility of Sr and Ca in the cubic structure of ZrO_2 has been reported.[5,6] The different solubility of Sr and Ca in YSZ at 1200°C can be explained due to the larger ionic radius of Sr^{2+} (1.31 Å) compared to that of Ca^{2+} (1.18Å), which is revealed in the chemical composition analysis of phases by EDX presented in Table 3.

Table 2
The analysis results of B-site cation valence, oxygen content, thermogravimetric analysis and differential thermal analysis for $La_{0.6}M_{0.4}Mn_{0.8}Co_{0.2}O_{3-\delta}$ (M = Sr and Ca)

M in $La_{0.6}M_{0.4}Mn_{0.8}Co_{0.2}O_{3-\delta}$	Sr	Ca
$B^{4+}/(B^{3+}+B^{4+})$ (%)	37.8	39.3
$3-\delta$	2.989	2.996
Weight loss	No	No
Phase transformation	No	No

Table 3
EDX analysis of primary phases for powder mixtures annealed at 1200°C for 24 h[a]

Mixture	Phase	La	M	Mn	Co	Y	Zr
LSMC/YSZ	LSMC	28	12	36	7	2	15
	YSZ	–	–	4	2	21	73
LCMC/YSZ	LCMC	31	16	35	10	1	7
	YSZ	5	3	6	3	10	74

[a] LSMC = $La_{0.6}Sr_{0.4}Mn_{0.8}Co_{0.2}O_{3-\delta}$; LCMC = $La_{0.6}Ca_{0.4}Mn_{0.8}Co_{0.2}O_{3-\delta}$.

Therefore, the excess amount of Sr^{2+} precipitated at the boundaries. After the precipitation, Sr readily reacts with ZrO_2 in YSZ to produce $SrZrO_3$. The solubility of La_2O_3 in the $SrZrO_3$ layer was detected by other EDX investigations,[7] which can explain the lacking of La in YSZ, as indicated in Table 3.

The expansion and contraction of the YSZ lattice must be due to compositional changes in the cubic YSZ (solid solution), originating from diffusion of cations. With the smaller size of Mn^{4+} or Co^{4+} compared with that of Zr^{4+}, a lattice contraction will take place by the diffusion of the two kinds of cations. The contraction of the YSZ lattice has been reported in the literatures.[8,9] In the present study, however, the expansion of the YSZ lattice was observed for both the LSMC/YSZ and LCMC/YSZ mixtures, as shown in Fig. 2. With the diffusion of Mn^{4+} and Co^{4+} into the YSZ lattice for the LSMC/YSZ mixtures, a large amount of Zr^{4+} were consumed for the formation of $SrZrO_3$. The composition of the YSZ solid solution shifted to that with higher concentration of Y^{3+}. For the LCMC/YSZ mixtures, however, a significant amount of La^{3+} and Ca^{2+} also diffused into the YSZ lattice with the diffusion of Mn^{4+} and Co^{4+}. As a result, the total concentrations of Y^{3+}, La^{3+} and Ca^{2+} in the YSZ solid solution are higher than that of Y^{3+} in the pure YSZ lattice. The compositional changes were revealed by EDX, as indicated in Table 3. Therefore, the expansion behavior due to higher concentrations of cations with larger size dominated over the contraction behavior of Mn^{4+} and Co^{4+} in both the lattices of YSZ solid solutions.

It is well known that a high Sr content in perovskites results in the formation of $SrZrO_3$ in reaction with YSZ. $SrZrO_3$ is formed irrespective of the rare earth cation in $RE_{0.6}Sr_{0.4}Mn_{0.8}Co_{0.2}O_{3-\delta}$. However, the amounts of $SrZrO_3$ formed strongly depend on the rare earth radius, as shown in Fig. 3. These results are consistent with that reported by G.Ch Kostogloudis and Ch. Ftikos.[10] The different extent of $SrZrO_3$ formation can be discussed on the basis of disorder effects due to size difference between A-site RE^{3+} and Sr^{2+}, which is characterized by the weighted average A-site cation radius $<r_A>$. $<r_A>$ has been used to find the strong correlation with transition temperature between ferromagnetic metallic and paramagnetic insulating states in $RE_{1-x}M_xMnO_3$ perovskites.[11] When Sr is substituted for RE in $RE_{0.6}Sr_{0.4}Mn_{0.8}Co_{0.2}O_{3-\delta}$, the large radius of Sr^{2+}, compared to that of RE^{3+}, results in the distortion of coordination polyhedra in perovskite structure. As indicated by $<r_A>$ in Table 1, the distortion tends to be larger from La to Gd. According to the bond-valence model, the distortion effect then produced a stress in perovskite structure. In order to relieve the stress, a larger amounts of unstable Mn^{4+} and Co^{4+} diffused into the lattice of YSZ for perovskite with smaller rare earth radius. Therefore, larger amounts of Sr precipitated at the boundaries. As a result, more $SrZrO_3$ was formed when the precipitated Sr reacted with ZrO_2 in YSZ for the perovskite with smaller RE ionic radius.

5. Conclusion

The present studies have revealed that $RE_{0.6}M_{0.4}Mn_{0.8}Co_{0.2}O_{3-\delta}$ (RE = La, Pr, Nd, Sm and Gd; M = Sr and Ca) showed different compatibility towards YSZ at 1200°C. $SrZrO_3$ was formed as a reaction product for $RE_{0.6}Sr_{0.4}Mn_{0.8}Co_{0.2}O_{3-\delta}$. In contrary, there is no reaction product for $RE_{0.6}Ca_{0.4}Mn_{0.8}Co_{0.2}O_{3-\delta}$. It can be considered that the solubility of Ca in YSZ avoids the formation of $CaZrO_3$. The present studies also showed that larger disorder effect due to size difference between A-site RE^{3+} and Sr^{2+} resulted in larger amounts of $SrZrO_3$ formed in reaction. The perovskites in $RE_{0.6}Ca_{0.4}Mn_{0.8}Co_{0.2}O_3$ deserve further investigations on the chemical stability of the solid-state interface with YSZ for use as cathode materials in YSZ-based SOFC.

Acknowledgements

The authors wish to thank Dr. J.B. He for his support in EDX analysis.

References

1. Ishihara, T., Kudo, T., Matsuda, H. and Takita, Y., Doped perovskite oxide, $PrMnO_3$, as a new cathode for solid-oxide fuel cells that decreases the operating temperature. *J. Am. Ceram. Soc.*, 1994, **77**, 1682–1684.

2. Tu, H. Y., Phillipps, M. B., Takeda, Y., Ichikawa, T., Imanishi, N., Sammes, N. M. and Yamamoto, O., $Gd_{1-x}A_xMn_{1-y}Co_yO_{3-\delta}$ (A = Sr, Ca) as a cathode for solid oxide fuel cells. *J. Electrochem. Soc*., 1999, **146**, 2085–2091.
3. Shannon, R. D., Revised effective ionic radii and systematic studies of interatomic distances in halides and chalcogenides. *Acta. Cryst*., 1976, **A32**, 751–767.
4. Brown, I. D., Chemical and steric constraints in inorganic solids. *Acta Cryst*., 1992, **B48**, 553–572.
5. Noguchi, T. and Yonemochi, O., Reactions in the system ZrO_2-SrO. *J. Am. Ceram. Soc*., 1969, **52**, 178–181.
6. Duwez, P., Odell, F. and Brown, F. H. Jr, Stabilization of zirconia with calcia and magnesia.. *J. Am. Ceram. Soc*., 1952, **35**, 107–113.
7. Ivers-Tiffeé, E., Schieβl, M., Oel, H. J. and Wersing, W., Investigations of cobalt-containing perovskites in SOFC single cells with respect to interface reactions and cell performance. In *Proceedings of the 3rd International Symposium on Solid Oxide Fuel Cells*, ed. S. C. Singhal and H. Iwahara, Hawaii, 1933, pp. 613–622.
8. Wiik, K., Schmidt, C. R., Faaland, S., Shamsili, S., Einarsrud, M.-A. and Grande, T., Reactions between strontium-substituted lanthanum manganite and yttria-stabilized zirconia: powder samples. *J. Am. Ceram. Soc*., 1999, **82**, 721–728.
9. Kostogloudis, G. Ch., Tsiniarakis, G. and Ftikos, Ch., Chemical reactivity of perovskite oxide SOFC cathodes and yttria stabilized zirconia. In *Proceedings of the 12th International Conference on Solid State Ionics*, 6–12 June, 1999, Halkidiki, Greece, p. 227.
10. Kostogloudis, G. Ch. and Ftikos, Ch., Chemical compatibility of $Re_{1-x}Sr_xMnO_{3\delta}$(RE = La, Pr, Nd, Gd, $0 \leq x \leq 0.5$) with yttria stabilized zirconia solid electrolyte. *J. Eur. Ceram. Soc*., 1998, **18**, 1707–1710.
11. Rodriguez-Martinez, L. M. and Attfiels, J. P., Cation disorder and size effects in magnetoresistive manganese oxide perovskites. *Phys. Rev*., 1996, **B54**, R15622–R15625.